

Numerical analysis of wave propagation in fluid-filled deformable tubes

David Uribe^{1,2,*}, Holger Steeb², Erik H. Saenger³, Patrick Kurzeja¹, and Oscar Ruiz²

¹ Mechanics – Continuum Mechanics, Ruhr-University Bochum, Germany

² CAD/CAM/CAE Laboratory, Universidad EAFIT, Medellín, Colombia

³ Geological Institute, ETH Zürich, Switzerland

The theory of Biot describing wave propagation in fluid saturated porous media is a good effective approximation of a wave induced in a fluid-filled deformable tube. Nonetheless, it has been found that Biot's theory has shortcomings in predicting the fast P-wave velocities and the amount of intrinsic attenuation. These problems arises when complex mechanical interactions of the solid phase and the fluid phase in the micro-scale are not taken into account. In contrast, the approach proposed by Bernabe does take into account micro-scopic interaction between phases and therefore poses an interesting alternative to Biot's theory. A Wave propagating in a deformable tube saturated with a viscous fluid is a simplified model of a porous material, and therefore the study of this geometry is of great interest. By using this geometry, the results of analytical and numerical results have an easier interpretation and therefore can be compared straightforward. Using a Finite Difference viscoelastic wave propagation code, the transient response was simulated. The wave source was modified with different characteristic frequencies in order to gain information of the dispersion relation. It was found that the P-wave velocities of the simulations at sub-critical frequencies closely match those of Bernabe's solution, but at over-critical frequencies they come closer to Biot's solution.

Copyright line will be provided by the publisher

1 Introduction

According to Biot's theory ([1, 2]) low frequency acoustic wave propagation across porous media is dominated by viscosity (Poiseuille flow). At high frequencies, the viscosity loses significance and the fluid separates from the solid walls. As a consequence, two P-waves coexist, and the wave at the fluid side has the form of plug flow. Likewise, Bernabe's approach ([5]) has two characteristic frequency domains. The ranges of these domains match those proposed by Biot. A difference in their approaches can be seen in their equations of momentum equilibrium. Biot suggests that the equilibrium condition is fulfilled at the macro-scale, but Bernabe's equations point to an equilibrium at the micro-scale. Furthermore, the constitutive relations of Biot have material properties involving the macro and micro-scale, however, Bernabe focuses on material properties only in the micro-scale.

The dispersion relation is the raion between the wave speeds of a propagating wave against its frequency. We will compare the dispersion relations of Biot's theory, Bernabe's theory and the numerical simulation, and conclude which theory is more appropriate for each frequency domain.

2 Methodology

2.1 Analytical solutions

Eq. (1) is the simplified dispersion characteristic polynomial ([3]) with roots ξ_1 and ξ_2 . From the relation $k_{1,2}^2 = \xi_{1,2}$, it is possible to find the wave number k . The values of the parameters N, A, Q, R, P are effective material parameters that can be determined by laboratory experiments. The P-wave velocities follow from $c = \omega/\text{Re}(k)$.

In Bernabe's solution, the characteristic polynomial is given by eq. (2), with $J_i(\cdot)$: Bessel function of the first kind, c_f : wave speed the fluid phase, c_s^S : wave speed in the solid phase, ρ^{fR} : fluid phase density and ρ^{sR} : solid phase density.

$$0 = [PR - Q^2]\xi^2 - [P\hat{\rho}_{22} + R\hat{\rho}_{11} - 2Q\hat{\rho}_{12}]\xi + [\hat{\rho}_{11}\hat{\rho}_{22} - \hat{\rho}_{12}\hat{\rho}_{12}], \quad (1)$$

$$0 = c^4 - c^2 \left(\frac{2J_1(kr)}{krJ_0(kr)} \frac{\rho}{\rho^{sR}} c_F^2 + c_F^2 + 2c_s^{S2} \right) + 2c_s^{S2} c_F^2 \left(1 - \frac{2J_1(kr)}{krJ_0(kr)} \right) \quad (2)$$

2.2 Numerical approximation

The geometry of the elastic tube is discretized using a regular three dimensional grid. The inner radius is $r = 0.25$ mm and the outer radio is $R = 0.7$ mm. The material properties of the solid phase are $c_s^P = 5330$ m/s, $c_s^S = 3145$ m/s, $\rho^{sR} = 7900$ kg/m³

* Corresponding author: e-mail david.uribe@rub.de, phone +49 234 32 23078, fax +49 234 32 14229

(similar to those of steel). The properties of the fluid phase are $c_f = 1920$ m/s, $\rho^{fR} = 1258$ kg/m³ and $\eta^{fR} = 1.412$ Pa · s (glycerol under standard conditions).

The time domain is discretized using a second-order finite difference operator. The spatial derivatives are approximated by fourth-order finite difference operators using a rotated staggered grid (RSG). The time and spatial discretization are solved explicitly in the code. The elastodynamic wave equations, extended by anelastic functions, eqs. (3), are solved with the finite difference method. In order to enforce the viscoelastic properties of the fluid phase, the approach of [4] is used implementing the anelastic coefficient tensor \tilde{Y}_m^{ijkl} . Other approximations of the anelastic coefficient tensor appear in [6–8]. The elastic tube is loaded at one end of the tube with a planar wave. The induced wave is a first time derivative of a normal distribution with a characteristic frequency f_c .

$$\sigma_{ij} = C_{ijkl}\varepsilon_{kl} - \sum_m^{ij} \xi_m^{ij}, \quad \dot{\xi}_m^{ij} + \omega_m \xi_m^{ij} = \omega_m \tilde{Y}_m^{ijkl} \varepsilon_{kl}. \quad (3)$$

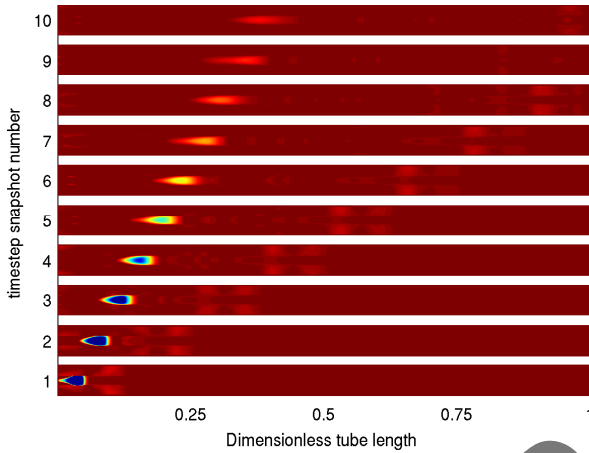


Fig. 1: Cross sectional view of the propagating wave in the middle plane along the axial direction. $f_c = 150$ kHz.

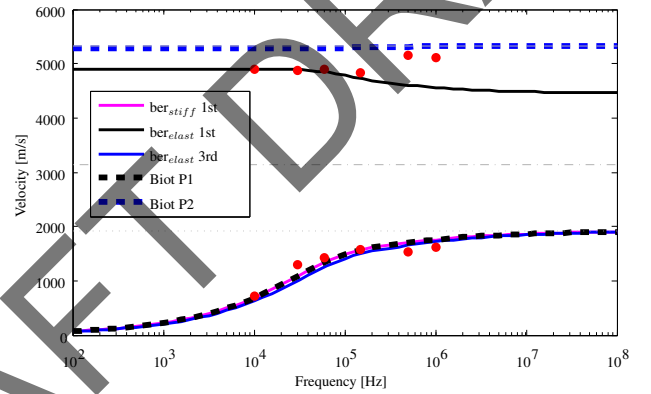


Fig. 2: Dispersion relation (from Biot, Bernabe and numerical solutions). The red dots indicate the phase velocities from the simulations.

3 Results

The numerical simulation represents and clearly depicts the microscopic flow process in Fig. 1. Phase velocities can be derived from the first arrivals of the waves between two time steps. It can be seen that at sub-critical frequencies, the numerical results are closer to Bernabe's solution, Fig 2. At over-critical frequencies the numerical results resemble Biot's solution. It is observed that in the high frequency domain, the flow is indeed that of a plug flow.

4 Conclusions and Future work

We compare here the wave propagation models by Biot and Bernabe by using a finite differences approach. In the low frequency domain, the approach of Bernabe is more accurate predicting the phase velocities. In the high frequency domain, Biot's model is better to calculate the phase velocities. Future work aims to compare the velocity profile of the fluid phase between the numerical simulations and the analytical solutions, simulation of 2 and 3 dimensional lattices and the simulation of viscous solid materials.

References

- [1] M. A. Biot. J. Acoust. Soc. Am. **28**, 168 (1956).
- [2] M. A. Biot. J. Acoust. Soc. Am. **28**, 179 (1956).
- [3] H. Steeb. Arch. Appl. Mech. **80**, 489 (2010).
- [4] E. H. Saenger, S. A. Shapiro, and Y. Keehm. Geo. Res. Letters. **32**, 14 (2005).
- [5] Y. Bernabe. Rock Physics and Nat. Hazards 969 (2009).
- [6] J. M. Carcione. Geo. Phys. Int. **28**, 168 (1990).
- [7] H. Emmerich. Geo. **80**, 489 (2010).
- [8] P. Moczo, J. Kristek, and P. Franke. Lecture notes on rheological models. (2006).